Universal size-dependent conductance fluctuations in disordered organic semiconductors

Universal Size-Dependent Conductance Fluctuations in Disordered Organic Semiconductors

A. Massé,[1] R. Coehoorn,[2,1] and P. A. Bobbert[1]
[1]Department of Applied Physics, Eindhoven University of Technology, P.O. Box 513, 5600 MB Eindhoven, Netherlands
[2]Philips Research Laboratories, High Tech Campus 4, 5656 AE Eindhoven, Netherlands
(Received 6 June 2014; published 11 September 2014)

Numerically exact results of hopping charge transport in disordered organic semiconductors show for uncorrelated and dipole-correlated Gaussian energy disorder a universal, power-law, and non-power-law dependence, respectively, of the relative conductance fluctuations on the size of the considered region. Data collapse occurs upon scaling with a characteristic length having a power-law temperature dependence. Below this length, which can be as high as 100 nm for correlated disorder in a realistic case, fluctuations dominate and a continuum description of charge transport breaks down.

DOI: 10.1103/PhysRevLett.113.116604 PACS numbers: 72.20.Ee, 72.80.Le, 72.80.Ng

Disordered organic semiconductors are the crucial element in organic devices like organic light-emitting diodes (OLEDs). Charge transport in these materials occurs by hopping of charge carriers between localization sites with random on-site energies. Percolation theories have been employed to describe this transport and to obtain the dependence of the charge-carrier mobility μ on temperature T, carrier concentration c, and electric field F [1–7]. The presently standard approach in organic device modeling is to use $\mu(T, c, F)$ in continuum drift-diffusion calculations of charge transport [8].

There are, however, at least three reasons to critically analyze the validity of such a continuum approach. (i) Present-day OLEDs, and in particular white OLEDs, have sublayers of only a few nanometers thick [9,10]. It is questionable if such thin layers can still be considered as a continuum. (ii) A continuum approach to charge transport in disordered media will fail when the size of the considered region is below a critical size where sample-to-sample fluctuations in the conductance are no longer negligible. (iii) For the spatial correlation in the energetic disorder believed to be present in small-molecule semiconductors [8], these fluctuations are expected to be even more prominent than without correlation. An analysis of the conditions at which a continuum approach breaks down and of the character of charge transport under such conditions is therefore of utmost importance.

In this Letter, we perform such an analysis. We focus on the widely used Gaussian disorder model (GDM) and the correlated disorder model (CDM) for site-energy disorder. In the GDM, proposed by Bässler, the disorder is modeled by a Gaussian distribution of uncorrelated on-site energies [11]. In the CDM, the energetic disorder is assumed to be caused by molecular dipoles with random orientation [12], creating a spatial correlation between on-site energies that decays with distance r as $1/r$ [13]. The GDM and CDM, extended to the EGDM [4] and ECDM [14] to account for the c dependence of μ in addition to the originally considered T and F dependence, are well applicable to charge transport in polymeric and small-molecule semiconductors, respectively [8].

Another important reason for our analysis is that several theory groups are studying charge transport in these semiconductors from a fundamental perspective, attempting to find realistic morphologies and hopping rates from atomistic studies [15–18]. Because of the involved computational costs, such studies necessarily involve relatively small systems. An important question is what the influence of this is on the calculated charge-transport properties. Lukyanov and Andrienko already noted that the calculated mobilities are strongly system size dependent. They propose to find the room-temperature mobility by extrapolation of mobilities calculated at higher temperatures, where finite-size effects are smaller, to room temperature [19].

Here, we analyze for small F the sample-to-sample fluctuations in the conductance G of a cubic simulation box with side L for different disorder configurations. If the relative fluctuations are sufficiently small, transport in the box represents that in a homogeneous medium. An important question is at what minimum size of the box this is the case. The behavior of the fluctuations themselves provides important information about charge transport in confined situations, such as a thin organic layer in an OLED or a small simulation box in the case of atomistic studies. In analyzing fluctuations, in the case of percolative charge transport the specific boundary conditions are not important [2], and we therefore choose computationally convenient periodic boundary conditions. To investigate possible influences of the lattice type, we consider simple cubic (SC) and fcc lattices. We define a length unit $a \equiv N_t^{-1/3}$, where N_t is the site density. At most one charge carrier can be present at a lattice site due to strong on-site Coulomb repulsion, which is the most important effect of Coulomb interactions at the carrier concentrations $c < 0.01$ we will

consider (higher concentrations are seldom reached in organic devices). The c dependence of μ was found to be more important than the F dependence in charge-transport modeling of hole-only polymer devices [4], so that the small-F limit considered here is very relevant. In this limit, an exact mapping onto a random-resistor network can be made [6], where every resistor represents a bond between two sites.

We consider Miller-Abrahams (MA) [20] as well as Marcus [21] hopping rates ω_{ij} between nearest-neighbor sites i and j, since these types of rates have been mostly used in the literature. For MA hopping from i to j, $\omega_{ij} = \omega_0 \exp(-[\Delta E_{ij} + |\Delta E_{ij}|]/2k_BT)$, with ω_0 a prefactor, ΔE_{ij} the energy difference between sites j and i, including a contribution by the field F, and k_B Boltzmann's constant. For Marcus hopping, $\omega_{ij} = (J_0^2/\hbar)\sqrt{\pi/E_r k_B T}\exp(-[\Delta E_{ij} + E_r]^2/4E_r k_B T)$, where J_0 is the charge-transfer integral and E_r the reorganization energy upon charging or discharging of the site due to nuclear rearrangements. The use of Marcus hopping rates has a stronger microscopic foundation [15] but needs specification of E_r. In materials for which $E_r \gg \Delta E_{ij}$ (indicated by $E_r \to \infty$ below), however, the E_r dependence of the rate appears only in the prefactor.

The master equation for the occupational probabilities p_i of the sites is solved numerically (see Supplemental Material [22]). From these, the currents across all bonds and the conductance G of the box can be calculated. Disorder configurations are generated by drawing random site energies from a Gaussian distribution with standard deviation σ (uncorrelated disorder) or by placing randomly oriented dipoles on the lattice sites and evaluating the resulting electrostatic energies at the sites (correlated disorder). Relations between the dipole moment and the resulting standard deviation σ of the density of states, which is very close to Gaussian, are given in Ref. [7] for the SC and fcc lattice.

We first consider uncorrelated disorder. To visualize the issues to be addressed, we show in Fig. 1 the bond current distribution in a two-dimensional (2D) square lattice for a representative case, for $\hat{\sigma} \equiv \sigma/k_BT = 3$ and 6. The relative sample-to-sample fluctuations in the conductance of a box in this lattice will increase with decreasing linear size L of the box. For the red boxes with characteristic size L_0, the fluctuations in the conductance are as large as the typical conductance itself. For smaller boxes, fluctuations become dominant. The important questions to be answered are as follows: how does L_0 depend on $\hat{\sigma}$, i.e., on temperature, and how does the size of the fluctuations depend on L?

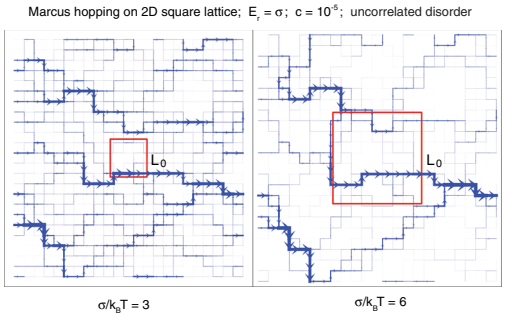

FIG. 1 (color online). Bond current distribution (arrows, directions; line thicknesses, sizes) for a representative 2D case with uncorrelated disorder, for two disorder strengths. At the size L_0 of the red boxes, conductance fluctuations are comparable to the conductance itself.

For all considered cases, the distribution of G is very close to log-normal, which can be rationalized from the exponential dependence of the hopping rates on the site energies. We therefore study the distribution of $\ln(G/G_0)$, where $G_0 \equiv \exp\langle \ln G\rangle$ ($\langle \ldots \rangle$ is a disorder average). For a representative three-dimensional (3D) case, Fig. 2(a) shows this distribution, which is very close to normal, for different box sizes L. We define $\delta(L)$ as the standard deviation of this distribution. Figure 2(b) shows G_0 vs a/L and a comparison to equivalent results for $G_0^C \equiv \langle G\rangle$ and $G_0^R \equiv \langle G^{-1}\rangle^{-1}$, corresponding to the average conductance and resistance, respectively. The results for G_0^C (G_0^R) lie significantly above (below) these for G_0, because of the skewness of the log-normal distributions (the distribution of the resistances $R = 1/G$ is also log-normal and has the same shape as that of G). It is clear from Fig. 2(b) that the macroscopic conductivity can be much more accurately obtained from G_0 than from G_0^C or G_0^R for calculations on small systems. Hence, this is an attractive route to calculate the macroscopic conductivity from simulations on small systems, providing an alternative to the "temperature-extrapolation" method of Ref. [19]. G_0^C can be considered as the conductance of a system of many boxes in parallel, corresponding to an organic layer in between two highly

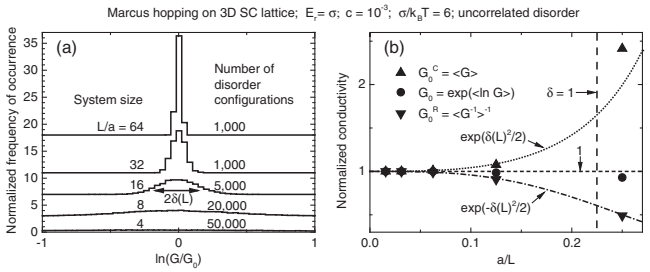

FIG. 2. (a) Normalized occurrence frequency of $\ln(G/G_0)$ of conductances of boxes with different size L (offsets applied), for a representative 3D case with uncorrelated disorder. The mean-square fluctuation $\delta(L)$ is indicated for one case. The bin size was 0.04, and the numbers of disorder configurations considered are given. (b) Conductivities vs a/L normalized to the macroscopic conductivity (dashed horizontal line), calculated from the data in (a): disorder averages of the conductance (G_0^C), resistance (G_0^R), and logarithm of the conductance (G_0). See the main text for the explanation of the functions $\exp[\delta(L)^2/2]$ and $\exp[-\delta(L)^2/2]$. At the vertical dashed line, $\delta(L) = \delta(L_0) = 1$. Errors in the data are smaller than the symbols.

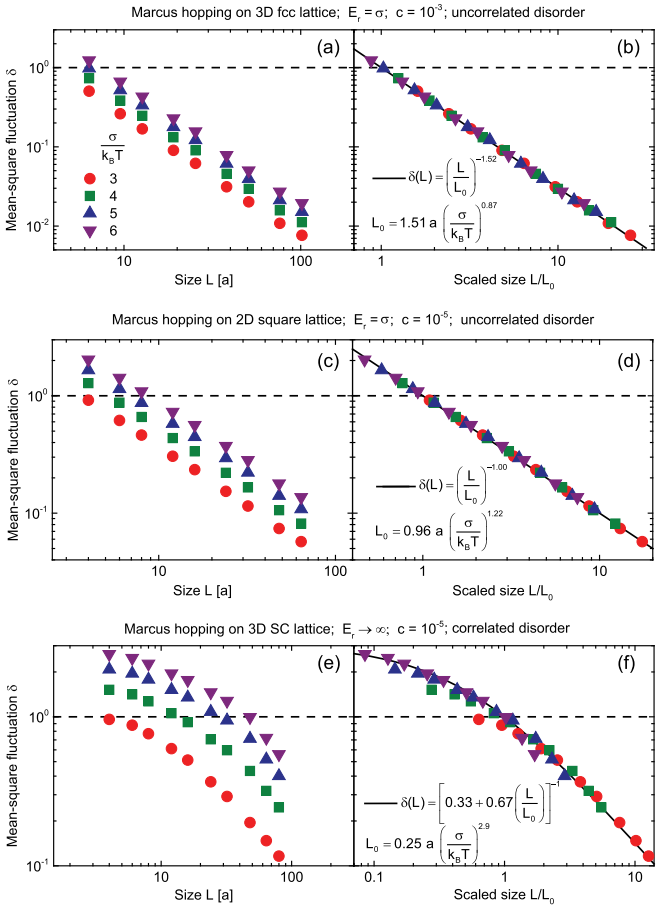

FIG. 3 (color online). Mean-square fluctuation δ vs box size L (left) and scaled size L/L_0 (right) for different disorder strengths and three different cases, corresponding to uncorrelated disorder in 3D [(a),(b)] and 2D [(c),(d)] and dipole-correlated disorder in 3D [(e),(f)]. Values of L_0 used in the size scaling are indicated and a parametrization of the curves according to Eqs. (1) and (2). Numbers of considered disorder configurations varied between 1000 (uncorrelated disorder) and 150 (correlated disorder) for the largest box to 50 000 (both cases) for the smallest box. Errors in the data are smaller than the displayed symbols.

conducting layers. The conductance can then be considerably higher than following from a continuum description.

For another representative 3D case, Fig. 3(a) shows $\delta(L)$ vs L for various values of $\hat{\sigma}$. We find for all $\hat{\sigma}$ a perfect power-law behavior $\delta(L) \propto (L/a)^{-\kappa}$. Furthermore, Fig. 3(b) shows that the curves of Fig. 3(a) perfectly collapse onto a master curve if L is scaled with a characteristic length $L_0 = Aa\hat{\sigma}^{\nu}$, where the numerical prefactor A is chosen such that $\delta(L_0) = 1$. For this system size, the fluctuations in G are comparable to G_0. Combining the two results leads to

$$\delta(L) = \left(\frac{L_0}{L}\right)^{\kappa} = \left(\frac{Aa\hat{\sigma}^{\nu}}{L}\right)^{\kappa}. \quad (1)$$

This behavior appears to be universal, since it is found not to depend on the type of hopping and lattice or on the carrier concentration. Table I shows fitted values of κ, ν, and A for a number of cases. Even the presence of traps, very relevant for electron transport in organic semiconductors [23] and for OLEDs making use of dyes [9,10], does not change this behavior [22]. The exponent κ is very close to 1.5 for all cases. In line with predictions from percolation theory [2], we find that the exponents ν in Table I are within the numerical accuracy equal to the percolation correlation-length exponent, which is $\nu = 0.875$ in 3D [24]. Also indicated in Fig. 2(b) are the functions $\exp[\delta(L)^2/2]$ and $\exp[-\delta(L)^2/2]$, corresponding to the normalized averages of the log-normal distributions of the conductance and resistance, respectively, using Eq. (1) and the results from Table I. They agree fairly well with the actual data and can therefore be used as a rule of thumb in estimating finite-size corrections.

It is interesting to also analyze the 2D case. Figures 3(c) and 3(d) show results equivalent to those of Figs. 3(a) and 3(b) for the 2D case considered in Fig. 1. The conclusions are similar. Again we find a power-law behavior $\delta(L) \propto (L/a)^{-\kappa}$, but now with an exponent $\kappa = 1.00 \pm 0.02$. The exponent ν is now 1.22 ± 0.02, which is close to the 2D percolation correlation-length exponent $\nu = 4/3$. Importantly, several data points are obtained for which $\delta > 1$, clearly showing that there is no change in behavior around $\delta = 1$. The red boxes in Fig. 1 have a size equal to the characteristic length $L_0 = 0.96a\hat{\sigma}^{1.22}$ at which $\delta = 1$.

The values for κ close to 1 in 2D and 3/2 in 3D suggest the relation $\kappa = D/2$, with D the dimension. In the limit $\delta \to 0$, this can be rationalized as follows. We can subdivide the box with size L into $N = (L/L')^D$ subboxes with size L'. When $\delta(L') \ll 1$, the distribution of conductances of the subboxes has become normal and very sharply peaked around the average conductance. In determining the conductance of the box with side L from the conductances of the subboxes, we can then linearize in the fluctuations of these conductances. Since these fluctuations are uncorrelated, we conclude that $\delta(L) = \delta(L')/\sqrt{N} = \delta(L')(L/L')^{-D/2}$, so that $\kappa = D/2$. Surprisingly, this power-law behavior also holds when the condition $\delta \ll 1$ is not satisfied. We note that our results deviate in important respects from the analyses of Shklovskii and Efros [2] and LeDoussal [25], as discussed in the Supplemental Material [22].

We now turn to the case of dipole-correlated disorder. The algebraic decay $1/r$ of the energy-energy correlation function, meaning that the disorder has no finite correlation length, makes this case particularly interesting. Hence, the standard percolation theory cannot be applied, but we can nevertheless attempt to apply the same procedures as above.

We find that, except for the smallest boxes considered, the distribution of G is again log-normal. Figure 3(e) shows results for $\delta(L)$ vs L for a representative case. Clearly, the L dependence is no longer a power law. However, we still

TABLE I. Values of κ, ν, and A found to bring data for different considered cases onto the master curve of Eq. (1), for 3D hopping with uncorrelated disorder.

Lattice	Hopping	$E_r[\sigma]$	c	κ	ν	A
SC	MA	N/A	10^{-5}	1.52 ± 0.01	0.86 ± 0.01	1.03 ± 0.01
SC	MA	N/A	10^{-3}	1.52 ± 0.01	0.86 ± 0.01	1.03 ± 0.01
SC	Marcus	∞	10^{-5}	1.52 ± 0.02	0.85 ± 0.01	0.97 ± 0.01
SC	Marcus	∞	10^{-3}	1.52 ± 0.02	0.85 ± 0.01	0.97 ± 0.01
SC	Marcus	1	10^{-5}	1.52 ± 0.01	0.85 ± 0.01	0.97 ± 0.01
SC	Marcus	1	10^{-3}	1.52 ± 0.01	0.85 ± 0.01	0.97 ± 0.01
fcc	MA	N/A	10^{-5}	1.53 ± 0.03	0.88 ± 0.02	1.60 ± 0.01
fcc	MA	N/A	10^{-3}	1.53 ± 0.02	0.89 ± 0.01	1.60 ± 0.01
fcc	Marcus	∞	10^{-5}	1.52 ± 0.03	0.87 ± 0.02	1.51 ± 0.01
fcc	Marcus	∞	10^{-3}	1.52 ± 0.03	0.87 ± 0.02	1.51 ± 0.01
fcc	Marcus	1	10^{-5}	1.52 ± 0.03	0.87 ± 0.02	1.51 ± 0.01
fcc	Marcus	1	10^{-3}	1.52 ± 0.03	0.87 ± 0.02	1.51 ± 0.01

obtain data collapse by scaling L with a length $L_0 = A' a \hat{\sigma}^{\nu'}$ for some power ν' and prefactor A'. If results for the smallest boxes are disregarded, we see in Fig. 3(f) that this is possible for $\nu' = 2.9 \pm 0.3$. Table II contains results for various considered cases, showing very similar values of ν'. We thus find for dipole-correlated disorder

$$\delta(L) = f\left(\frac{L}{L_0}\right) \approx \left[0.33 + 0.67 \frac{L}{A' a \hat{\sigma}^{\nu'}}\right]^{-1}, \qquad (2)$$

where the second equality gives an approximation to the master curve $f(x)$. We note that for $\delta \ll 1$ the decay $\delta(L) \propto (L/L_0)^{-1}$ with L in Eq. (2) is slower than $(L/L_0)^{-3/2}$. The reason is that, because of the $1/r$ spatial correlation in the disorder, fluctuations in the conductances of subboxes never become uncorrelated.

In the region $\delta > 1$ above the dashed lines in Fig. 3, fluctuations in the conductance are dominant. In this region, the conductance of a specific disorder config can deviate strongly from the average, and a continuum approach breaks down. For polymeric semiconductors, the values $\sigma = 0.14$ eV and $a = 1.6$–1.8 nm [4] were found from EGDM modeling of hole-only devices. At room temperature, we then have $\hat{\sigma} \approx 5.6$, and we estimate from Eq. (1), taking $A = 1$, that $\delta > 1$ below about $L = 8$ nm. At such layer thicknesses, a continuum approach breaks down, but also when the mobility varies significantly on this scale due to large gradients in the carrier density.

TABLE II. As in Table I, but for correlated disorder and using Eq. (2). The carrier concentration was in all cases $c = 10^{-5}$.

Lattice	Hopping	$E_r[\sigma]$	ν'	A'
SC	MA	N/A	2.8 ± 0.2	0.28 ± 0.02
SC	Marcus	∞	2.9 ± 0.3	0.25 ± 0.02
SC	Marcus	1	2.9 ± 0.2	0.25 ± 0.02
fcc	MA	N/A	2.8 ± 0.2	0.46 ± 0.03
fcc	Marcus	∞	2.9 ± 0.3	0.40 ± 0.02
fcc	Marcus	1	2.9 ± 0.2	0.40 ± 0.03

Another important example is Alq_3 [tris(8-hydroxyquinolinato)aluminium], a small-molecule semiconductor with a relatively large molecular dipole moment. Atomistic modeling yields $\sigma = 0.19$ eV [26]. Assuming correlated disorder, Eq. (2) predicts, by taking $A' = 0.25$, $a = 1$ nm, and $\nu' = 2.9$, that at room temperature fluctuations are dominant up to sizes of even 100 nm. This is of the order of the organic layer thickness in a typical single-layer OLED and much larger than the thickness of some organic layers used in multilayer OLEDs [9,10]. This example shows that a continuum approach to small-molecule organic device modeling can fail severely.

In conclusion, we found from numerically exact results that conductance fluctuations in disordered semiconductors show a universal size dependence. The results allow an assessment of the validity of a continuum approach to charge transport in these semiconductors under various conditions, showing that this approach can be insufficiently accurate for organic semiconductor device modeling under realistic conditions. In particular, a continuum approach can severely underestimate the conductance of a thin organic layer. We expect impact of our work in the area of charge transport in disordered media, in general.

We thank M. A. J. Michels for very helpful hints, J. Cottaar, A. V. Nenashev, F. Jansson, F. Gebhard, and S. D. Baranovskii for discussions that prompted this research, and L. Zhang for critically reading the manuscript. The research is supported by the Dutch Technology Foundation STW, applied science division of NWO, and the Technology Program of the Ministry of Economic Affairs.

[1] V. Ambegaokar, B. I. Halperin, and J. S. Langer, Phys. Rev. B **4**, 2612 (1971).

[2] B. Shklovskii and A. Efros, *Electronic Properties of Doped Semiconductors* (Springer-Verlag, Berlin, 1984), Chap. 5.

[3] S. Baranovskii, O. Rubel, and P. Thomas, Thin Solid Films **487**, 2 (2005).
[4] W. F. Pasveer, J. Cottaar, C. Tanase, R. Coehoorn, P. A. Bobbert, P. W. M. Blom, D. M. de Leeuw, and M. A. J. Michels, Phys. Rev. Lett. **94**, 206601 (2005).
[5] R. Coehoorn, W. F. Pasveer, P. A. Bobbert, and M. A. J. Michels, Phys. Rev. B **72**, 155206 (2005).
[6] J. Cottaar, L. J. A. Koster, R. Coehoorn, and P. A. Bobbert, Phys. Rev. Lett. **107**, 136601 (2011).
[7] J. Cottaar, R. Coehoorn, and P. A. Bobbert, Phys. Rev. B **85**, 245205 (2012).
[8] R. Coehoorn and P. A. Bobbert, Phys. Status Solidi A **209**, 2354 (2012).
[9] S. Reineke, F. Lindner, G. Schwartz, N. Seidler, K. Walzer, B. Lüssem, and K. Leo, Nature (London) **459**, 234 (2009).
[10] M. Mesta, M. Carvelli, R. J. de Vries, H. van Eersel, J. J. M. van der Holst, M. Schober, M. Furno, B. Lüssem, K. Leo, P. Loebl, R. Coehoorn, and P. A. Bobbert, Nat. Mater. **12**, 652 (2013).
[11] H. Bässler, Phys. Status Solidi B **175**, 15 (1993).
[12] Y. Gartstein and E. Conwell, Chem. Phys. Lett. **245**, 351 (1995).
[13] S. V. Novikov, D. H. Dunlap, V. M. Kenkre, P. E. Parris, and A. V. Vannikov, Phys. Rev. Lett. **81**, 4472 (1998).
[14] M. Bouhassoune, S. L. M. van Mensfoort, P. A. Bobbert, and R. Coehoorn, Org. Electron. **10**, 437 (2009).
[15] J. J. Kwiatkowski, J. Nelson, H. Li, J. L. Bredas, W. Wenzel, and C. Lennartz, Phys. Chem. Chem. Phys. **10**, 1852 (2008).
[16] N. Vukmirović and L.-W. Wang, Appl. Phys. Lett. **97**, 043305 (2010).
[17] V. Rühle, A. Lukyanov, F. May, M. Schrader, T. Vehoff, J. Kirkpatrick, B. Baumeier, and D. Andrienko, J. Chem. Theory Comput. **7**, 3335 (2011).
[18] Y. Olivier, D. Niedzialek, V. Lemaur, W. Pisula, K. Müllen, U. Koldemir, J. R. Reynolds, R. Lazzaroni, J. Cornil, and D. Beljonne, Adv. Mater. **26**, 2119 (2014).
[19] A. Lukyanov and D. Andrienko, Phys. Rev. B **82**, 193202 (2010).
[20] A. Miller and E. Abrahams, Phys. Rev. **120**, 745 (1960).
[21] R. A. Marcus, Rev. Mod. Phys. **65**, 599 (1993).
[22] See Supplemental Material at http://link.aps.org/supplemental/10.1103/PhysRevLett.113.116604 for (1) solution of the master equation, (2) traps, (3) comparison with the analysis of Shklovskii and Efros, and (4) random-resistor network.
[23] H. T. Nicolai, M. Kuik, G. A. H. Wetzelaer, B. de Boer, C. Campbell, C. Risko, J. L. Brédas, and P. W. M. Blom, Nat. Mater. **11**, 882 (2012).
[24] C. D. Lorenz and R. M. Ziff, Phys. Rev. E **57**, 230 (1998).
[25] P. LeDoussal, Phys. Rev. B **39**, 881 (1989).
[26] B. Baumeier, O. Stenzel, C. Poelking, D. Andrienko, and V. Schmidt, Phys. Rev. B **86**, 184202 (2012).